

# Modeling the Rotation of Orthotropic Axes of Sheet Metals Subjected to Off-Axis Uniaxial Tension

Wei Tong

Hong Tao

Xiquan Jiang

Department of Mechanical Engineering,  
Yale University,  
219 Becton Center,  
New Haven, CT 06520-8284

*A simplified version of a newly developed anisotropic plasticity theory is presented to describe the anisotropic flow behavior of orthotropic polycrystalline sheet metals under uniaxial tension. The theory is formulated in terms of the intrinsic variables of principal stresses and a loading orientation angle and its uniaxial tension version requires a non-quadratic stress exponent and up to five anisotropic material functions of the loading orientation angle to specify a flow condition, a flow rule for plastic strain rates, a flow rule for macroscopic plastic spin, and an evolution law of isotropic hardening. In this investigation, the proper analytical form and the associated parameter identification of the anisotropic material functions defining the flow rule of macroscopic plastic spin are discussed for sheet metals with persistent but rotated orthotropic symmetry axes under off-axis uniaxial tension. It is shown that the proposed flow rule of macroscopic plastic spin can successfully model the experimental data on the rotation of orthotropic symmetry axes in the three sheet metals reported, respectively, by Boehler et al. (Boehler and Koss, 1991, *Advances in Continuum Mechanics*, O. Bruller et al., eds., Springer, Heidelberg, pp. 143–158; Losilla, Boehler, and Zheng, 2000, *Acta Mech.* **144**, pp. 169–183); Kim and Yin (1997, *J. Mech. Phys. Solids* **45**, pp. 841–851); and Bunge and Nielsen (1997 *Int. J. Plasticity* **13**, pp. 435–446). [DOI: 10.1115/1.1755694]*

## 1 Introduction

The microstructure of a polycrystalline sheet metal generally evolves as it undergoes some finite plastic deformation. The plasticity-induced microstructural evolution occurs at least at two levels: the crystallographic texture evolution of grains and the dislocation substructure texture evolution within the grains. There have been continued efforts on improving phenomenological macroscopic plasticity theories by incorporating some constitutive modeling capabilities of material microstructural evolution using scalar and tensorial internal state variables. Isotropic strain or work hardening characterized by an effective plastic strain or equivalent specific plastic work, [1], is perhaps the best-known single scalar state variable model of material microstructural evolution (it basically accounts for the increase of the average dislocation density in a metal due to plastic flow). The kinematic hardening model with a backstress tensor developed for isotropic plasticity theories, [2–4], can be regarded as the phenomenological description of anisotropic hardening behavior due to the evolution of the dislocation substructure towards some preferred spatial orientations that are aligned with current plastic straining directions.

On the other hand, metal products manufactured by rolling (sheet metals), drawing (wires), and extrusion (plates) are typically anisotropic (primarily due to the resulting crystallographic texture, i.e., grains packed with some preferred orientations) and so the use of anisotropic plasticity theories is more appropriate in engineering design and analysis of these materials, [5–8]. While

many macroscopic anisotropic plasticity theories proposed in the literature have incorporated isotropic hardening and even kinematic hardening models developed originally for isotropic plasticity theories, almost all of them have explicitly or implicitly assumed that the initial material texture is strong and it persists upon further plastic straining, i.e., the evolution of crystallographic texture is not considered. However, both micromechanical analyses and experimental investigations of rolled sheet metals have shown that there are noticeable and even significant changes of material orthotropic symmetry when a sheet metal is subjected to a plastic strain up to 20%–30%, [9–12]. For two rolled steel and one aluminum sheet metals that were subjected to *off-axis* uniaxial tension (i.e., the axial loading direction is not aligned with the orthotropic axes of the sheets), experimental observations have shown that the orthotropic symmetry of these sheet metals is more or less intact but the symmetry axes rotate relatively with respect to the sheet metal itself in the plane of the sheet, [10–12]. A flow rule for macroscopic plastic spin (accounting for the orientational evolution of the material texture frame) may thus be appropriate in an anisotropic plasticity theory to describe these experimental observations.

The concept of macroscopic plastic spin has been explicitly introduced since early 1970s into the framework of polycrystalline plasticity theories, [13–15]. Considerable attentions have been devoted to its role from theoretical considerations (such as a missing kinematics link to the material microstructural evolution) and the necessity from the standpoint of the stability of numerical simulations, [16–34]. The flow rule of macroscopic plastic spin proposed in the literature are mainly motivated and derived through either the representation theorems or some heuristic micromechanical arguments involving tensorial structure variables, identified to be either the orthotropic or other privileged material frames or back stress tensors. Only very simple analytical forms of the flow rule of macroscopic plastic spin have been suggested for illustrative purpose, mostly for either von Mises quadratic isotropic plasticity theory with tensorial backstress kinematic hardening

Contributed by the Applied Mechanics Division of THE AMERICAN SOCIETY OF MECHANICAL ENGINEERS for publication in the ASME JOURNAL OF APPLIED MECHANICS. Manuscript received by the Applied Mechanics Division, February 28, 2003; final revision, September 3, 2003. Associate Editor: M.-J. Pindera. Discussion on the paper should be addressed to the Editor, Prof. Robert M. McMeeking, Journal of Applied Mechanics, Department of Mechanical and Environmental Engineering, University of California–Santa Barbara, Santa Barbara, CA 93106-5070, and will be accepted until four months after final publication in the paper itself in the ASME JOURNAL OF APPLIED MECHANICS.

or Hill's 1948 quadratic anisotropic plasticity theory with isotropic hardening and strong and persistent orthotropic symmetry. Nevertheless, the existing simple flow rules of macroscopic plastic spin for orthotropic sheet metals are found to be unable to describe consistently the rotation of orthotropic axes observed in experiments, [11,28].

In this investigation, a flow rule of macroscopic plastic spin proposed in a newly developed anisotropic plasticity theory, [35–40] is evaluated for modeling the rotation of orthotropic symmetry axes in the two steel and one aluminum sheet metals subjected to off-axis uniaxial tension. First, constitutive equations of the anisotropic plasticity theory along with the procedure on evaluating anisotropic material functions in these constitutive equations are summarized in Section 2 for polycrystalline sheet metals under uniaxial tension. The experimental investigations on the orientational evolution of orthotropic symmetry axes in sheet metals are briefly reviewed and material parameters of the anisotropic material functions defining the flow rule of macroscopic plastic spin proposed in the theory are identified in Section 3. Results of both the experimental measurements and the model descriptions are compared for the three sheet metals in Section 3 as well. A discussion on the proper formulation and the necessity of the flow rule of macroscopic plastic spin for modeling the anisotropic plastic flow of sheet metals is presented in Section 4. Conclusions drawn from this investigation on modeling macroscopic plastic spin are given in Section 5.

## 2 A Model of Anisotropic Plastic Flows Under Uniaxial Tension

The finite elastic-plastic deformation kinematics of a sheet metal may be expressed through the multiplicative decomposition of the macroscopic deformation gradient tensor  $\mathbf{F}$  into the elastic and plastic parts  $\mathbf{F}^e$  and  $\mathbf{F}^p$ , [31]. By neglecting the small elastic stretching in sheet metals involving finite plastic deformation, one has the commonly known results of rigid-viscoplastic deformation kinematics as follows:

$$\begin{aligned}\mathbf{F} &= \mathbf{F}^e \mathbf{F}^p \approx \mathbf{R}^* \mathbf{F}^p, \\ \mathbf{L} &= \dot{\mathbf{F}} \mathbf{F}^{-1} \approx (\dot{\mathbf{R}}^* \mathbf{F}^p + \mathbf{R}^* \dot{\mathbf{F}}^p) \mathbf{F}^{p-1} \mathbf{R}^{*-1} \\ &= \dot{\mathbf{R}}^* \mathbf{R}^{*-1} + \mathbf{R}^* \dot{\mathbf{F}}^p \mathbf{F}^{p-1} \mathbf{R}^{*-1},\end{aligned}\quad (1)$$

$$\begin{aligned}\mathbf{L} &= \mathbf{D} + \mathbf{W} \approx \mathbf{D}^p + \mathbf{W}^* + \mathbf{W}^p, \\ \mathbf{D} &= (\mathbf{L} + \mathbf{L}^T)/2 = \mathbf{D}^e + \mathbf{D}^p \approx \mathbf{D}^p, \\ \mathbf{W} &= (\mathbf{L} - \mathbf{L}^T)/2 = \mathbf{W}^* + \mathbf{W}^p,\end{aligned}\quad (2)$$

where  $\mathbf{R}^*$  is the rigid body rotation of the underlying material "texture" frame (some preferred orientations such as orthotropic symmetry axes),  $\mathbf{D}^p$  is the plastic rate of deformation tensor,  $\mathbf{W}^p$  is the plastic spin tensor defined as the difference between the material spin  $\mathbf{W}$ , and the so-called constitutive spin  $\mathbf{W}^*$ , [17,28]. A complete macroscopic theory of plastic flow usually provides a flow condition, flow rules that define both the plastic strain rate tensor  $\mathbf{D}^p$  and the plastic spin rate tensor  $\mathbf{W}^p$ , and isotropic and even anisotropic hardening models via a set of internal state variables and associated kinetic equations on their evolution, [32–34].

Using the principal axes of the applied stress tensor as the Cartesian coordinate system of the choice in this investigation (see Fig. 1), the expressions for the stress tensor  $\boldsymbol{\sigma}$ , the macroscopic plastic rate of deformation tensor  $\mathbf{D}^p$ , the macroscopic plastic spin tensor  $\mathbf{W}^p$ , and the material constitutive spin tensor  $\mathbf{W}^*$  under *uniaxial tension* are

$$\boldsymbol{\sigma} = \begin{pmatrix} \sigma_\theta & & \\ & 0 & \\ & & 0 \end{pmatrix}, \quad \mathbf{D}^p = \begin{pmatrix} \dot{\epsilon}_1 & \dot{\epsilon}_{12} & 0 \\ \dot{\epsilon}_{21} & \dot{\epsilon}_2 & 0 \\ 0 & 0 & \dot{\epsilon}_3 \end{pmatrix},$$

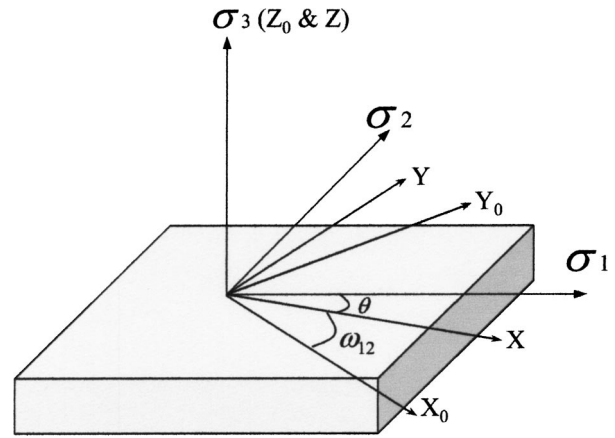


**Fig. 1** Definitions of the three Cartesian coordinate systems for a monoclinic sheet metal: (a) the principal axes of stress ( $\sigma_1, \sigma_2, \sigma_3$ ); (b) the principal axes of the current material texture frame  $XYZ$ ; and (c) the sheet material coordinate system  $X_0 Y_0 Z_0$ . The principal axis of  $\sigma_3$  always coincides with  $Z_0$ -axis and  $Z$ -axis to ensure the planar plastic flow of the sheet metal. The in-plane axes  $X$  and  $Y$  of the texture frame are defined to be the principal straining directions of the sheet metal under equal biaxial tension ( $\sigma_1 = \sigma_2, \sigma_3 = 0$ ). The material coordinate system  $X_0 Y_0 Z_0$  undergoes the same rigid body rotation as the sheet metal itself and it may be chosen to coincide with the initial texture frame of the sheet metal (the initial texture frame of an orthotropic sheet metal is defined by its rolling (RD), transverse (TD), and normal (ND) directions). The loading orientation angle  $\theta$  is defined as the angle between the principal axis of  $\sigma_1$  and the  $X$ -axis of the material texture frame. The relative rotation  $\omega_{12}$  of the texture frame with respect to the material coordinate system of the sheet metal is due to the macroscopic plastic spin  $\dot{\omega}_{12}$ , [28].

$$\mathbf{W}^p = \begin{pmatrix} 0 & \dot{\omega}_{12} & 0 \\ \dot{\omega}_{21} & 0 & 0 \\ 0 & 0 & 0 \end{pmatrix}, \quad \mathbf{W}^* = \begin{pmatrix} 0 & \dot{\omega}_{12}^* & 0 \\ \dot{\omega}_{21}^* & 0 & 0 \\ 0 & 0 & 0 \end{pmatrix}, \quad (3)$$

where  $\theta$  is the *loading orientation angle* defined as the angle between the axial loading direction  $\sigma_1 = \sigma_\theta > 0$  and the current in-plane  $X$ -axis of the sheet metal texture frame (see Fig. 1), and

$$\begin{aligned}\dot{\epsilon}_3 &= -\dot{\epsilon}_1 - \dot{\epsilon}_2, & \dot{\epsilon}_{21} &= \dot{\epsilon}_{12}, & \dot{\omega}_{21} &= -\dot{\omega}_{12}, \\ \dot{\omega}_{21}^* &= -\dot{\omega}_{12}^*, & \dot{W}_{12} &= \dot{\omega}_{12}^* + \dot{\omega}_{12},\end{aligned}\quad (4)$$

where  $\dot{W}_{12}$  is the in-plane material spin (macroscopically observable) of the sheet metal. We propose the following rate-dependent phenomenological theory to model the anisotropic plastic flow of a sheet metal under *uniaxial tension*

$$\tau = \tau_0(\xi, \dot{\gamma}),$$

$$\tau^a = \sigma_\theta^a \Phi_1(\theta) \quad (\text{the flow condition and flow function}), \quad (5)$$

$$\dot{\epsilon}_1 = \dot{\gamma} \left( \frac{\sigma_\theta}{\tau} \right)^{a-1} \Phi_1(\theta), \quad \dot{\epsilon}_2 = \dot{\gamma} \left( \frac{\sigma_\theta}{\tau} \right)^{a-1} \Phi_2(\theta),$$

$$\dot{\epsilon}_{12} = \dot{\gamma} \left( \frac{\sigma_\theta}{\tau} \right)^{a-1} \Phi_3(\theta), \quad (\text{the flow rule for } \mathbf{D}^p) \quad (6)$$

$$\dot{\omega}_{12} = \dot{\gamma} \left( \frac{\sigma_\theta}{\tau} \right)^{a-1} \Phi_4(\theta), \quad (\text{the flow rule for } \mathbf{W}^p) \quad (7)$$

$$\dot{\xi} = \dot{\gamma} \left( \frac{\Phi_5(\theta)}{\Phi_1(\theta)} \right)^{a-1/a}$$

(the evolution law of isotropic hardening), (8)

where  $\tau$  is the effective flow stress,  $\dot{\gamma}$  is the work-conjugate effective plastic strain rate,  $\xi$  is a certain internal state variable characterizing the isotropic hardening state of the material,  $\tau_0$  is the effective flow strength,  $a (> 1)$  is the stress exponent and it is a noninteger in general, and  $\Phi_1(\theta)$ ,  $\Phi_2(\theta)$ ,  $\Phi_3(\theta)$ ,  $\Phi_4(\theta)$ , and  $\Phi_5(\theta)$  are five material functions characterizing the planar plastic anisotropy of the sheet metal under uniaxial tension. The constitutive equations Eqs. (5)–(8) are the simplified (uniaxial tension) version of a planar anisotropic plastic flow theory recently developed by Tong et al. [35–40] in terms of principal stresses and a loading orientation angle (which have been called intrinsic variables of a stress field according to Hill [41,42]). The above constitutive equations under uniaxial tension can be justified from a micromechanical point of view (see Appendix). When the associated flow rule is applied to  $\dot{\epsilon}_{12}$ , [41,42], one has  $\Phi_3(\theta) = \Phi_1'(\theta)/2a$ . If one assumes  $\Phi_5(\theta) = \Phi_1(\theta)$ , then  $\dot{\xi} = \dot{\gamma}$ , i.e., the isotropic hardening is characterized by the cumulative effective plastic strain. On the other hand, if one assumes  $\Phi_5(\theta) = \Phi_1(\theta) \tau^{a/(a-1)}$ , then  $\dot{\xi} = \tau \dot{\gamma}$ , i.e., the isotropic hardening is characterized by the cumulative plastic work per unit volume.

Because the equivalence of the loading orientation angles of  $\theta$  and  $\theta \pm \pi$  due to the symmetry of mechanical loading, each of the five anisotropic material functions of a sheet metal can be represented by a Fourier series, namely,

$$\begin{aligned} \Phi_1(\theta) &= A_0 + A_1 \sin 2\theta + A_2 \cos 2\theta + \dots + A_{2k-1} \sin 2k\theta \\ &\quad + A_{2k} \cos 2k\theta + \dots, \\ \Phi_2(\theta) &= B_0 + B_1 \sin 2\theta + B_2 \cos 2\theta + \dots + B_{2k-1} \sin 2k\theta \\ &\quad + B_{2k} \cos 2k\theta + \dots, \\ \Phi_3(\theta) &= C_0 + C_1 \sin 2\theta + C_2 \cos 2\theta + \dots + C_{2k-1} \sin 2k\theta \\ &\quad + C_{2k} \cos 2k\theta + \dots, \\ \Phi_4(\theta) &= D_0 + D_1 \sin 2\theta + D_2 \cos 2\theta + \dots + D_{2k-1} \sin 2k\theta \\ &\quad + D_{2k} \cos 2k\theta + \dots, \\ \Phi_5(\theta) &= E_0 + E_1 \sin 2\theta + E_2 \cos 2\theta + \dots + E_{2k-1} \sin 2k\theta \\ &\quad + E_{2k} \cos 2k\theta + \dots, \end{aligned} \quad (9)$$

where  $k = 1, 2, \dots$ , and  $A_n$ ,  $B_n$ ,  $C_n$ ,  $D_n$ , and  $E_n$  are the Fourier coefficients. The stress exponent  $a$  and the Fourier coefficients of the five anisotropic material functions in Eq. (9) may evolve with subsequent plastic deformation when anisotropic hardening due to material texture evolution is modeled. They are all assumed to be constant in this investigation, i.e., the characteristics of the material texture remains more or less the same but the whole texture frame can rotate relatively with respect to the sheet metal itself. If the sheet metal has some additional symmetry characteristics such as orthotropic, trigonal, or cubic symmetry in the plane of the sheet, one can reduce the number of terms in each Fourier series by imposing the equivalency of loading conditions between  $\theta$  and  $-\theta$ ,  $\theta$  and  $\theta + 2\pi/3$ , and  $\theta$  and  $\theta + \pi/2$  respectively. Furthermore, a truncated Fourier series may be used in practice to approximate each anisotropic material function and the number of terms kept in each truncated Fourier series depends on planar anisotropy of the sheet metal. Besides flow stress-strain curves  $\sigma_\theta(\epsilon_1, \dot{\epsilon}_1)$ , plastic strain and spin ratios can be measured under uniaxial tension:

$$R_\theta \equiv \frac{\dot{\epsilon}_2}{\dot{\epsilon}_3} = - \frac{\Phi_2(\theta)}{\Phi_1(\theta) + \Phi_2(\theta)}, \quad (\text{the plastic axial strain ratio}) \quad (10a)$$

$$\Gamma_\theta \equiv \frac{\dot{\epsilon}_{12}}{\dot{\epsilon}_1} = \frac{\Phi_3(\theta)}{\Phi_1(\theta)}, \quad (\text{the plastic shear strain ratio}) \quad (10b)$$

$$\Pi_\theta \equiv \frac{\dot{\omega}_{12}}{\dot{\epsilon}_1} = \frac{\Phi_4(\theta)}{\Phi_1(\theta)}. \quad (\text{the plastic spin ratio}). \quad (10c)$$

The five anisotropic material functions  $\Phi_1(\theta)$ ,  $\Phi_2(\theta)$ ,  $\Phi_3(\theta)$ ,  $\Phi_4(\theta)$ , and  $\Phi_5(\theta)$  in the proposed anisotropic plastic flow theory under uniaxial tension can thus be completely examined from the experimental measurements of  $\sigma_\theta(\epsilon_1, \dot{\epsilon}_1)$ ,  $R_\theta$ ,  $\Gamma_\theta$ , and  $\Pi_\theta$ , [35–37,40]. Evaluation of the proper analytical form of the anisotropic material function  $\Phi_4(\theta)$  that defines the flow rule of macroscopic plastic spin or the plastic spin ratio  $\Pi_\theta$  for a given sheet metal is the focus of this investigation and will be discussed in details in the next section.

### 3 Macroscopic Plastic Spin in Sheet Metals Subjected to Off-Axis Uniaxial Tension

In this section, the procedures of experimental investigations on the orientational evolution of material texture frames in three sheet metals will be reviewed first and the reported experimental results will be summarized briefly. The Fourier series representation and the identification of its Fourier coefficients of the anisotropic material function  $\Phi_4(\theta)$  or the plastic spin ratio  $\Pi_\theta$  will then be detailed. The model description of the rotation of orthotropic axes of these three sheet metals under off-axis uniaxial tension due to macroscopic plastic spin will be compared with the experimental measurements. Although the theory presented in Section 2 can be applied to monoclinic sheet metals under uniaxial tension, [37,40], the sheet metals considered in the following are assumed to be initially orthotropic and remain so under off-axis uniaxial tension, [11,28]. So only the coefficients of the sine terms in the Fourier series of  $\Phi_4(\theta)$  and the coefficients of the cosine terms in the Fourier series of  $\Phi_1(\theta)$  are nonzero.

**3.1 On the Experimental Measurements of the Rotation of Orthotropic Axes due to Macroscopic Plastic Spin.** There have been rather limited experimental investigations on detecting the macroscopic plastic spin and its evolution in orthotropic sheet metals so far, [10–12,43,44]. A direct *mechanistic* evaluation of the macroscopic plastic spin in orthotropic sheet metals under uniaxial tension has been carried out using a two-step experimental technique by Boehler and Koss [10] and Kim and Yin [11]. It consists of (a) *the plastic deformation step* of uniaxial straining multiple large sheet samples up to various plastic strain levels (10%–30%) without necking at different off-axis angles and (b) *the material (texture frame) probing step* of measuring the directional dependence of uniaxial tension flow stress (more specifically, the yield stress with a big offset strain of 0.2%) of smaller tensile sheet samples cut off from the deformed large sheet with every 10 deg or 15 deg offset angle increments from the original rolling direction.

Boehler et al. [10,45] tested large sheets of an aluminum killed soft steel of size  $1000 \times 360 \text{ mm}^2$  under uniaxial tension with initial off-axis loading orientation angles of 30 deg, 45 deg, and 60 deg for various plastic strain levels up to 20% and above. Twelve smaller specimens cut off from each of the deformed large sheets with angles of 0 deg, 15 deg, 30 deg, 45 deg, 60 deg, 75 deg, 90 deg, 105 deg, 120 deg, 135 deg, 150 deg, 165 deg offset from the rolling direction of the sheets were then tested for yield stress measurements. Kim and Yin [11] carried out very similar tests on an automotive low carbon steel sheet using the same three initial off-axis loading orientation angles for various strain levels up to 10%. They used a total of 18 smaller specimens cut off from each of the deformed large sheets in the material probing step with each specimen at an offset angle of every 10 deg increment from the rolling direction of the large sheets. To enhance the degree of anisotropy of the steel sheets that were nearly isotropic initially, Kim and Yin [11] pre-strained the steel sheets along the rolling direction up to strains of 3% and 6%, respectively. By examining the directional dependence of flow stress measured from 12 and 18 small tensile specimens, respectively, both Boehler et al.

[10,45] and Kim and Yin [11] concluded that their sheet metals remain approximately orthotropic but there exists a large in-plane rotation of the orthotropic symmetry axes relative to the sheet metal itself under off-axis uniaxial tension. Both positive (counterclockwise) and negative (clockwise) rotations as defined in Fig. 1 were observed for initial loading orientation angles of 30 deg and 60 deg, respectively, and the orthotropic symmetry axes become completely aligned with the external axial loading direction within 5–10% uniaxial plastic strain. That is, the texture axis that is coincided with the initial rolling direction rotates towards the axial loading direction with an initial loading orientation angle of 30 deg but the texture axis that is coincided with the initial transverse direction rotates towards the axial loading direction with an initial loading orientation angle of 60 deg. A rotation of the orthotropic symmetry axes with an initial loading orientation angle of 45 deg was detected in both investigations as well but a positive rotation was reported by Boehler and Koss [10] while a negative rotation was found by Kim and Yin [11].

An experimental determination of macroscopic plastic spin of polycrystals based on material crystallographic texture measurements has been proposed by Bunge and Nielsen [12]. They divided the crystallographic texture change of a polycrystal undergoing plastic deformation into an average rotation of some common texture reference axes characteristic for the whole polycrystal material element and a “spreading” of the individual crystal orientations away from the common (rotated) reference texture frame. When the texture “spreading” is neglected, the texture evolution can thus be characterized approximately by the texture rotation or texture spin. Bunge and Nielsen [12] measured the orientation distribution function (ODF) of an annealed polycrystalline aluminum sheet of 1 mm thickness before and after being subjected to off-axis uniaxial tension to a total plastic strain of 20% at 11 different initial loading orientation angles. They analyzed the rotation of a characteristic reference system formed by the symmetric elements of the texture with an accuracy of  $\sim 0.5$  deg using an autocorrelation function of ODF and considered the texture rotation or spin being related to the macroscopic plastic spin in the macroscopic theories of plasticity. They found that the amount of texture rotation at a uniaxial plastic strain of 20% depends on the initial loading orientation angle and the maximum plastic spin ratio is about 5 deg/20% occurred around the off-axis loading angle of 22.5 deg (i.e.,  $\Pi_{22.5\text{deg}} \approx 5$  deg/20% if a constant plastic spin is assumed). The macroscopic plastic spin of the aluminum sheet defined by the crystallographic texture spin according to Bunge and Nielsen [12] is much smaller than that of low-carbon steel sheets defined by the symmetry characteristics of the directional dependence of flow stress according to Boehler and Koss [10] and Kim and Yin [11]. Measured pole figures of a steel sheet investigated by Boehler and Koss [10] under 45 deg off-axis uniaxial tension showed that the symmetry part of the crystallographic texture in the steel sheet did rotate completely towards the axial loading direction at a plastic strain level of about 10%.

**3.2 An Analysis of the Rotation of Orthotropic Axes due to Macroscopic Plastic Spin.** As there is very little relative rotation of the sheet metal with respect to the fixed laboratory loading frame under uniaxial tension, [10–12,43,44], i.e.,  $\dot{W}_{12} \approx 0$ , one has (see Fig. 1)

$$\omega_{12} + \theta \approx \theta_0, \quad \text{and} \quad \dot{\omega}_{12} + \dot{\theta} \approx 0, \quad (11)$$

where  $\theta_0$  and  $\theta$  are, respectively, the initial and current loading orientation angles, and  $\omega_{12}$  is the rotation of the sheet metal texture frame due to plastic spin  $\dot{\omega}_{12}$ . One can thus rewrite Eq. (10c) as

$$\Pi_{\theta} = -\frac{\dot{\theta}}{\dot{\varepsilon}_1} \quad \text{or} \quad \varepsilon_1 = -\int_{\theta_0}^{\theta} \frac{d\theta}{\Pi_{\theta}}. \quad (12)$$

The directional dependence of flow stress under uniaxial tension is usually much milder than that of plastic strain and spin ratios.

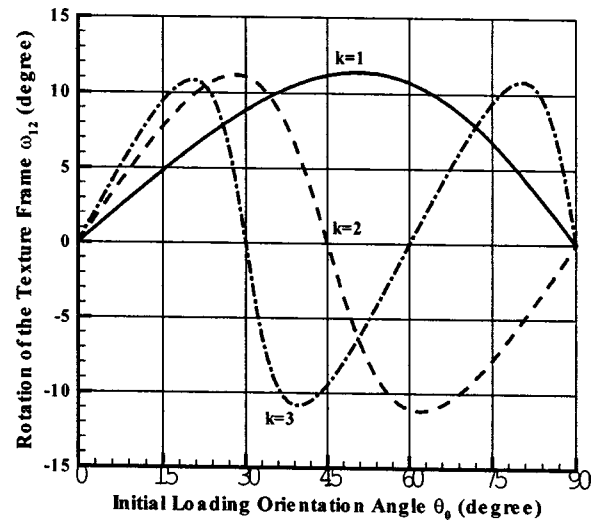


**Fig. 2 The amount of rotation  $\omega_{12}$  of the material texture frame due to plastic spin at a fixed uniaxial plastic strain  $\varepsilon_1$  of 20% as a function of the initial loading orientation angle  $\theta_0$  with three different  $k$  values according to Eq. (13b) ( $D=1$  is used for all data points)**

To the first approximation, one may set  $\Phi_1(\theta) \approx 1$  (assuming  $\tau(\xi, \dot{\gamma}) = \sigma_0$ ). When only one of coefficients in the Fourier series of  $\Phi_4(\theta)$  is nonzero, i.e.,  $\Pi_{\theta} \approx \Phi_4(\theta) \approx D \sin 2k\theta$  ( $k=1, 2, \dots$ ), one can obtain an analytical expression of Eq. (12) as

$$\theta = \frac{1}{k} \arctan[\{\tan(k\theta_0)e^{-2kD\varepsilon_1}\}], \quad (13a)$$

so

$$\omega_{12} = \theta_0 - \frac{1}{k} \arctan[\{\tan(k\theta_0)e^{-2kD\varepsilon_1}\}]. \quad (13b)$$

The rotation  $\omega_{12}$  of the material texture frame with respect to the sheet metal itself or the current loading orientation angle  $\theta$  as a function of the initial loading orientation angle  $\theta_0$  and the uniaxial plastic strain  $\varepsilon_1$  ( $\geq 0$ ) are shown in Fig. 2 and Fig. 3, respectively, using Eq. (13). The material texture frame will eventually stop spinning at certain loading orientation angles at sufficiently large plastic strains and these loading orientation angles are the *equilibrium* orientations of the material texture frame. Possible equilibrium orientations of the material texture frame of a sheet metal are the loading orientation angles that satisfy the conditions  $\Pi_{\theta} = 0$  and  $\Pi'_{\theta} \geq 0$ . Loading orientation angles that satisfy the conditions  $\Pi_{\theta} = 0$  and  $\Pi'_{\theta} < 0$  are metastable orientations and are not true equilibrium orientations (i.e., any small disturbance can cause the material texture frame to rotate away from those orientations). When  $D > 0$ , the possible equilibrium orientations of the material texture frame are  $\theta = 0$  deg for  $k=1$ ,  $\theta = 0$  deg and 90 deg for  $k=2$ , and  $\theta = 0$  deg, 60 deg and 120 deg for  $k=3$ . When  $D < 0$ , the possible equilibrium orientations of the material texture frame are  $\theta = 90$  deg for  $k=1$ ,  $\theta = 45$  deg and 135 deg for  $k=2$ , and  $\theta = 30$  deg, 90 deg, and 150 deg for  $k=3$ . In general, Eq. (12) may also be rewritten using the Fourier series expansion of  $\Pi_{\theta} = \Phi_4(\theta)/\Phi_1(\theta)$  as

$$\varepsilon_1 = -\int_{\theta_0}^{\theta} \frac{d\theta}{(d_1 \sin 2\theta + d_2 \sin 4\theta + d_3 \sin 6\theta + \dots)}. \quad (14)$$

The relation between the current loading orientation angle  $\theta$  or the rotation of the texture frame  $\omega_{12}$  and the uniaxial plastic strain  $\varepsilon_1$  can be obtained by integrating Eq. (14) numerically.

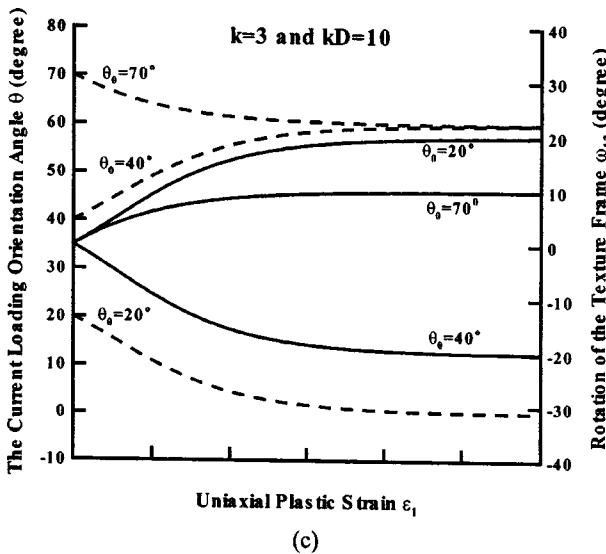
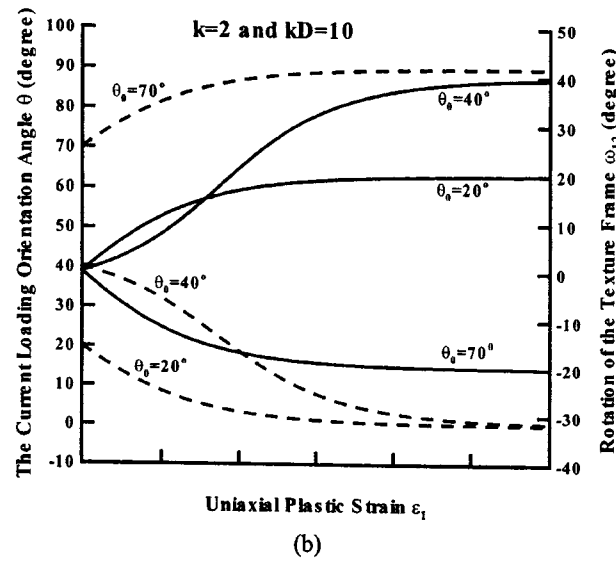
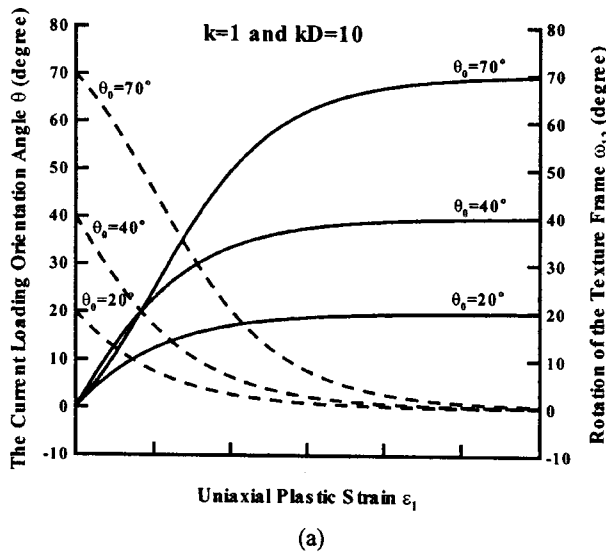


Fig. 3 The current loading orientation angle  $\theta$  and the amount of rotation  $\omega_{12}$  of the material texture frame due to plastic spin as a function of uniaxial plastic strain  $\epsilon_1$  with three different initial loading orientation angles  $\theta_0$  and three different  $k$  values according to Eq. (13) ( $kD=10$  is used for all data points)

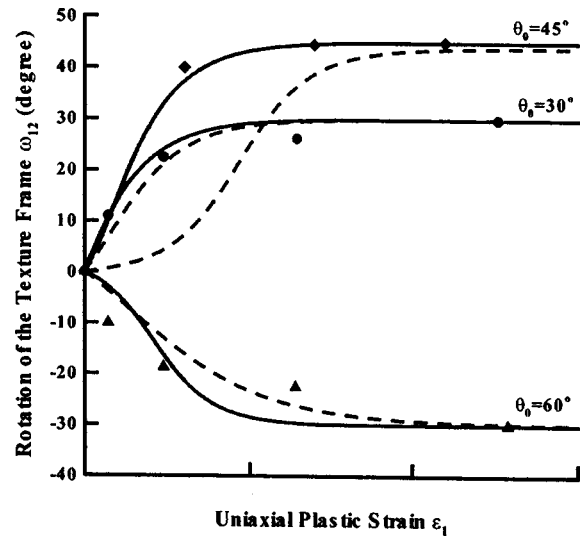


Fig. 4 Comparison of the model description (solid and dashed lines) and the experimental data (filled symbols) of a steel sheet reported by Boehler and Koss [10] and Losilla et al. [45] on the rotation  $\omega_{12}$  of the material texture frame due to plastic spin as a function of uniaxial plastic strain  $\epsilon_1$  with different initial loading orientation angles  $\theta_0=30\text{deg}$ ,  $45\text{deg}$ , and  $60\text{deg}$ . The solid lines are given by Eq. (14) with  $d_1=7$ ,  $d_2=10$  and  $d_3=-3$  (all other coefficients are zero). The dashed lines are given by Eq. (13b) with  $k=2$  and  $D=9$  (the initial loading orientation angles of  $30\text{deg}$ ,  $46\text{deg}$ , and  $60\text{deg}$  were used).

3.3 Comparison Between the Model Description and Experimental Measurements on the Rotation of Orthotropic Axes. Unlike plastic axial and shear strain ratios  $R_\theta$  and  $\Gamma_\theta$  (see Eqs. (10a) and (10b)) that can be directly determined from incremental plastic strain measurements in each uniaxial tension test, the plastic spin ratio has to be determined from the measurements of both axial plastic strain increments and rotations of the material symmetry axes (by a separate mechanical or material texture measurement, see Section 3.1). Only limited experimental data are reported for a given sheet metal either in terms of the rotation of orthotropic axes as a function of uniaxial plastic strain with selected initial loading orientation angles (see Fig. 4 and Fig. 5) or in terms of the rotation of crystallographic texture symmetry axes as a function of initial loading orientation angles at a fixed uniaxial plastic strain (see Fig. 6). The plastic spin ratio can be obtained in principle by curve-fitting and numerical differentiation of the experimental data shown in Fig. 4 and Fig. 5, the material parameters and coefficients in Eq. (13b) and/or Eq. (14) can then be determined. The following trial-and-error procedure is used instead for parameter identification:

1. Use the results shown in Fig. 2 and Fig. 3 (which are given by Eq. (13) using different  $k$  values) as the basis to determine the dominant term (the value of  $k$ ) in the Fourier series of  $\Pi_\theta$  measured in experiments.
2. Adjust the value of the coefficient  $D$  (both its sign and magnitude) to best describe the experimental data. If Eq. (13) with the selected values of  $k$  and  $D$  can model all of the experimental measurements reasonably well, then the plastic spin ratio is determined as  $\Pi_\theta = D \sin 2k\theta$ .
3. Add one or more sine terms for the Fourier series of  $\Pi_\theta$  if Eq. (13) cannot describe the experimental measurements satisfactorily. Estimate the sign and magnitude of the Fourier coefficient of each new term by comparing the results shown in Fig. 2 and Fig. 3 with the experimental measurements. Adjust the Fourier coefficients  $d_i$  in Eq. (14) iteratively until

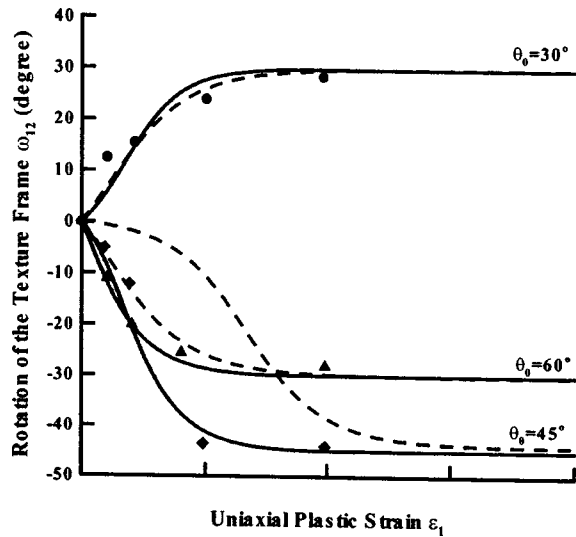


Fig. 5 Comparison of the model description (solid and dashed lines) and the experimental data (filled symbols) of a steel sheet reported by Kim and Yin [11] on the rotation  $\omega_{12}$  of the material texture frame due to plastic spin as a function of uniaxial plastic strain  $\varepsilon_1$  with different initial loading orientation angles  $\theta_0=30\text{deg}$ ,  $45\text{deg}$ , and  $60\text{deg}$ . The solid lines are given by Eq. (14) with  $d_1=-8$ ,  $d_2=17$  and  $d_3=3$  (all other coefficients are zero). The dashed lines are given by Eq. (13b) with  $k=2$  and  $D=12.5$  (the initial loading orientation angles of  $30\text{deg}$ ,  $46\text{deg}$ , and  $60\text{deg}$  were used).

the model description matches closely the experimental measurements. The plastic spin ratio is then given as  $\Pi_\theta = d_1 \sin 2\theta + d_2 \sin 4\theta + d_3 \sin 6\theta + \dots$

The above procedure was applied to model the experimental data on the three sheet metals reported by Boehler et al. [10,45], Kim and Yin [11], and Bunge and Nielsen [12] and plastic spin ratios of these three sheet metals were determined as follows:

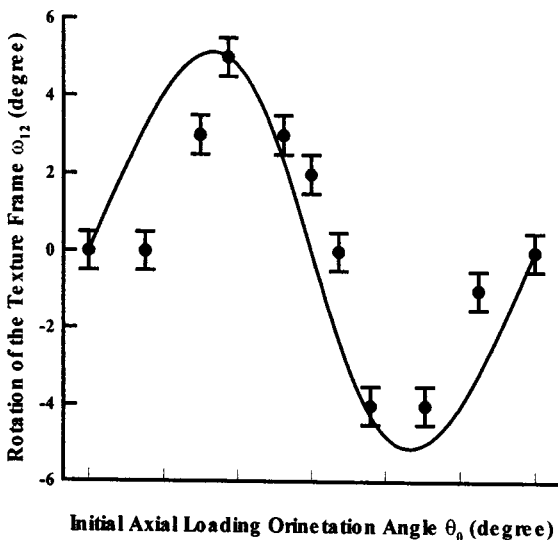


Fig. 6 Comparison of the model description (solid and dashed lines) and the experimental data (filled symbols) of an aluminum sheet reported by Bunge and Nielsen [12] on the amount of rotation  $\omega_{12}$  of the material texture frame due to plastic spin at a fixed uniaxial plastic strain  $\varepsilon_1$  of 20% with 11 different initial loading orientation angles  $\theta_0$ . The solid line is given by Eq. (13b) with  $k=2$  and  $D=0.45$ .

$$\Pi_\theta = 9 \sin 4\theta, \quad \text{and} \quad \Pi_\theta = 7 \sin 2\theta + 10 \sin 4\theta - 3 \sin 6\theta, \quad (\text{Boehler and Koss}) \quad (15a)$$

$$\Pi_\theta = 12.5 \sin 4\theta, \quad \text{and} \quad \Pi_\theta = -8 \sin 2\theta + 17 \sin 4\theta + 3 \sin 6\theta, \quad (\text{Kim and Yin}) \quad (15b)$$

$$\Pi_\theta = 0.45 \sin 4\theta \quad (\text{Bunge and Nielsen}). \quad (15c)$$

As shown in Fig. 4 and Fig. 5, the plastic spin ratio using a single sine term with  $k=2$  can only describe some of the experimental data on the two steel sheets reported by Boehler and Koss [10] and Kim and Yin [11] (for initial loading orientation angles of  $30\text{deg}$  and  $60\text{deg}$ ). Actually, no rotation of the orthotropic axes is predicted by  $\Pi_\theta = D \sin 4\theta$  for the initial loading orientation angle of  $45\text{deg}$  at all. However,  $\theta_0=45\text{deg}$  is not one of the true equilibrium orientations of the material texture frame with such a plastic spin ratio (see Section 3.2). If one assumes the initial loading orientation angle to be  $44\text{deg}$  and  $46\text{deg}$ , respectively, for each investigation (say, there were some experimental errors due to some slight misalignments), then the rotation of orthotropic axes occurs in both cases and matches the experimental observations at large strains. The predictions at small strains are however inconsistent with the experimental data. Indeed, the plastic spin ratios with three sine terms given in Eq. (15a) and Eq. (15b) are needed to adequately model the experimental data reported by both Boehler and Koss [10] and Kim and Yin [11] for all three different initial loading orientation angles. On the other hand, the plastic spin ratio using a single sine term with  $k=2$  describe reasonably well the directional dependence of the rotation of texture symmetry axes at a fixed uniaxial plastic strain of 20% as observed by Bunge and Nielsen [12] for an annealed aluminum sheet. The magnitude of the plastic spin ratio of the aluminum sheet is, however, about 1/20 to 1/30 of that of the steel sheets. The difference in the magnitude of plastic spin ratios between steel and aluminum sheets may be due to the difference in the characteristics of their initial anisotropy and a further micromechanical investigation is warranted to elucidate its physical origin. According to the plastic spin ratios given in Eq. (15), the equilibrium orientation of the material texture frames in these three sheet metals is either  $\theta=0\text{deg}$  (the X-axis will eventually coincide with the external axial loading direction) or  $\theta=90\text{deg}$  (the Y-axis will eventually coincide with the external axial loading direction).

#### 4 Discussion

A plane-stress anisotropic plasticity theory of sheet metals is often formulated using the Cartesian stress components  $\sigma_x$ ,  $\sigma_y$ , and  $\sigma_{xy}$  projected onto the principal axes of the material texture (symmetry) frame XYZ as shown in Fig. 1. Hill [41,42] has recently advocated the use of the so-called intrinsic variables of principal stresses ( $\sigma_1, \sigma_2$ ) and a loading orientation angle  $\theta$  for developing anisotropic plasticity theories. He has argued that the resulting plasticity theories should be more appealing to both theoreticians and experimentalists. A new anisotropic plasticity theory has indeed been proposed using these intrinsic variables by Tong et al. [35–40] and the uniaxial tension version of the theory is presented in this investigation. In both theoretical analyses and experimental evaluations of an anisotropic plasticity theory using either formulation, one needs to know the initial orientation of the material texture frame and its subsequent evolution with respect to the sheet metal itself during a plastic deformation process. In other words, an explicit mechanistic definition (i.e., an experimental procedure for its determination by a mechanical test) of the material texture frame at a given plastic deformation stage is required by such an anisotropic plasticity theory. For orthotropic sheets, the orthotropic axes can be identified with the symmetry axes detected in the orientational dependence of mechanical properties such as flow stress under uniaxial tension, [10,11]. If plastic anisotropy of the sheet metal is solely due to the crystallographic texture, then the crystallographic texture symmetry axes may be

used as well to measure the orientation of the material texture frame in the sheet metal, [12]. While such a definition of the material texture frame works well for sheet metals with orthotropic or other higher-order symmetries, it cannot however be extended to monoclinic sheets. A different and more general definition of the in-plane axes  $X$  and  $Y$  of the sheet material texture frame coordinate system has been given in the anisotropic plasticity theory presented here, that is, the  $X$  and  $Y$ -axes are defined to be the principal axes of in-plane plastic strain rates of the sheet metal under equal biaxial tension ( $\sigma_1 = \sigma_2$ ). In practice, an out-of-plane uniaxial compression test may be used to experimentally determine the material texture axes  $X$  and  $Y$  if plastic flow is unaffected by hydrostatic loading. This definition of the material texture axes is equivalent to the one based on the symmetry characteristics of flow stress under uniaxial tension for orthotropic sheets with isotropic hardening but requires much less experimental efforts, [35].

Most of the existing anisotropic plasticity theories assume that a polycrystalline sheet metal is orthotropic initially and the initial orthotropy symmetry is strong and persists during subsequent plastic deformation, [6,28]. When the sheet metal deforms plastically under on-axis loading conditions (i.e., the principal axes of stress coincide with the orthotropic axes of the sheet), there is no ambiguity on the orientation of the current orthotropic texture frame with respect to the sheet metal itself as there is no plastic spin of the material texture frame. However, when the loading is off-axis in uniaxial tension or shear tests, the original RD and TD directions of the sheet metal are no longer orthogonal and the current orientation of the material texture axes  $X$  and  $Y$  cannot be clearly identified without additional theoretical hypotheses or experimental characterization. Few existing anisotropic plasticity theories offer a flow rule for macroscopic plastic spin at all so most of them assume explicitly or implicitly that the macroscopic plastic spin is always zero and the material texture frame rotates along with the sheet metal itself. The experimental measurements on the current orientation of the material texture frame after a sheet metal is subjected to off-axis uniaxial tension have shown that there exist detectable and even significant relative rotations between the material texture frame and the sheet metal, [10–12]. A robust and flexible flow rule of macroscopic plastic spin as proposed in this investigation should be incorporated into an anisotropic plasticity theory to improve its modeling capabilities. A comparative evaluation of the proposed flow rule of macroscopic plastic spin with some of the specific analytical forms of the flow rule of macroscopic plastic spin appeared in the literature is in order. As pointed out in the Section 1, the explicit forms of the flow rule of macroscopic plastic spin have been motivated largely by invoking the representation theorems for isotropic functions in conjunction with the concept of tensorial structure variables mostly for quadratic plastic flow theories, [13–30]. Only two analytical expressions of the flow rule of macroscopic plastic spin have often been cited in the literature and they have the following forms for an orthotropic sheet metal under off-axis uniaxial tension, [28],

$$\dot{\omega}_{12} = \eta_a \dot{\epsilon}_{xy},$$

$$\begin{aligned} \text{or } \Pi_{\theta} &\equiv \frac{\dot{\omega}_{12}}{\dot{\epsilon}_1} \\ &= \eta_a \frac{(\dot{\epsilon}_1 - \dot{\epsilon}_2) \sin \theta \cos \theta + \dot{\epsilon}_{12} \cos 2\theta}{\dot{\epsilon}_1} \\ &= \eta_a \left[ \left( 1 + \frac{R_{\theta}}{1 + R_{\theta}} \right) \sin \theta \cos \theta + \Gamma_{\theta} \cos 2\theta \right], \quad (16a) \end{aligned}$$

$$\dot{\omega}_{12} = \eta_b \sigma_{\theta} \dot{\epsilon}_{12}, \quad \text{or } \Pi_{\theta} \equiv \frac{\dot{\omega}_{12}}{\dot{\epsilon}_1} = \eta_b \sigma_{\theta} \Gamma_{\theta}, \quad (16b)$$

where  $\eta_a$  and  $\eta_b$  are plastic spin coefficients and can be in general a function of the isotropic invariants of a given loading stress tensor and the material symmetry orientations,  $R_{\theta}$ ,  $\Gamma_{\theta}$ , and  $\sigma_{\theta}$  are, respectively, the plastic axial strain ratio, the plastic shear strain ratio, and the flow stress under uniaxial tension (see Section 2). The flow rule Eq. (16b) is the uniaxial tension version of the constitutive equation for plastic spin  $\mathbf{W}^p = \eta(\boldsymbol{\sigma} \mathbf{D}^p - \mathbf{D}^p \boldsymbol{\sigma})$  that has been adapted widely in the literature, [26–28]. In many actual applications of the above two flow rules reported in the literature, a constant plastic spin coefficient is usually assumed, [18,28]. The flow rule given by Eq. (16a) has been used extensively for investigating the plastic spin effect but they were mostly illustrative without experimental corroboration, [15,18]. The flow rule given by Eq. (16b) has been employed by Kuroda [26] to simulate the inverse Swift effect in free-end torsion experiments assuming that the material is orthotropic prior to torsion. Kim and Yin [11] and Dafalias [28] have used the same expression for the plastic spin along with Hill's 1948 quadratic anisotropic plasticity theory, [5], to simulate the orientational evolution of orthotropic symmetry axes in steel sheets upon off-axis uniaxial tensile deformation. While qualitative agreements were found in their analyses, the orientational evolution of the orthotropic axes with increasing plastic deformation is not described with great accuracy and significantly different values of the plastic spin coefficient  $\eta_b$  (which also has to be opposite in sign when comparing with the one used by Kuroda [26]) were needed for the best description of each of the off-axis tensile tests with the initial loading orientation angles of 30 deg, 45 deg, and 60 deg. In the light of the anisotropic plastic flow theory proposed here (see Section 2 and Section 3), the two widely used analytical expressions for the flow rule of macroscopic plastic spin as given in Eqs. (16a) and (16b) for uniaxial tension are indeed both overly restrictive (linking directly the plastic spin  $\dot{\omega}_{12}$  with the plastic shear rate  $\dot{\epsilon}_{xy}$  or  $\dot{\epsilon}_{12}$ ) and overly simplistic (no dependence on the loading orientation angle  $\theta$  is given for the plastic spin coefficients  $\eta_a$  and  $\eta_b$  at all in their actual application examples). The micromechanical analysis of the plastic flow of single crystals with a regularized Schmid law under uniaxial tension given in the Appendix also shows that the general validity of the plastic spin equation given by either Eq. (16a) or Eq. (16b) is indeed questionable.

As mentioned in the Introduction, the other major area of interest of incorporating a flow rule of macroscopic plastic spin is in isotropic plasticity theories with kinematic hardening [23,46]. One can define the material texture frame as the principal axes of the backstress tensor, then a flow rule of macroscopic plastic spin becomes basically a part of the evolution law of kinematic hardening that describes the orientational evolution of the principal axes of the backstress tensor (the other part covers the evolution of the strength of the backstress in terms of its principal components). However, direct measurements of the backstress tensor (and hence its principal axes) using tension-compression or similar tests at different loading orientation angles are required to properly evaluate any specific form of the flow rule of plastic spin for kinematic hardening. Experimental inference of the form of the flow rule of plastic spin for isotropic plasticity theories with kinematic hardening by simulating finite deformation simple shear tests is problematic [46] as the crystallographic aspect of the material texture evolution may become significant and even dominant. As observed early in Section 3, the magnitude of the plastic spin ratio of the aluminum sheet, [12], is only about 1/20 to 1/30 of that of the steel sheets, [10,11]. Such a difference may be attributed to the two different plastic spin detection methods used: the plastic spin determined by Bunge and Nielsen [12] is mainly related to the material crystallographic texture evolution while the plastic spin determined by Boehler and Koss [10] and Kim and Yin [11] may be related primarily to the evolution of dislocation substructures in steel sheet metals (especially at small plastic strains). In this investigation, it was assumed that all three sheet metals have a pre-existing orthotropic symmetry and the orienta-

tional dependence of flow stress and plastic strain ratio of the sheet metals under off-axis uniaxial tension remains orthotropic with the *same* symmetry axes, [28]. Consequently, a single macroscopic flow rule of macroscopic plastic spin was used to characterize satisfactorily the relative rotation of the material symmetry axes regardless of its origin. The validity of the persistent orthotropic symmetry assumption cannot be examined directly for these three sheet metals due to lack of experimental data. If the experimental data on the orientational dependence of plastic strain ratio of the two steel sheets upon off-axis uniaxial tension were also made available and they would show indeed that the symmetry axes of plastic strain ratio do not coincide with the symmetry axes of flow stress, the sheet metals should then be treated as monoclinic instead of orthotropic. Incorporations of both a backstress kinematic hardening model and a flow rule of macroscopic plastic spin in an anisotropic plastic flow theory may be a possible modeling approach, [23,43,44]. Direct experimental evaluation of the backstress tensor is however very challenging if not impossible for sheet metals (as in-plane uniaxial compression tests are rather difficult to carry out for thin sheets) and flow rules of two plastic spins are required to describe the orientation evolution of the principal axes of both the backstress (related primarily to the dislocation substructure) and the crystallographic texture frame, respectively, [23]. When only one plastic spin is used, its experimental evaluation becomes ambiguous unless further clarification on the definition of the material texture frame that is associated with the plastic spin is provided and extensive experimental data are made available. For example, Truong Qui and Lippmann [43,44] have proposed a quadratic anisotropic plasticity theory that generalizes Hill's orthotropic theory, [5], for monoclinic sheets with combined isotropic and kinematic hardening and a plastic spin. Their theory is formulated using the Cartesian stress components  $\sigma_x$ ,  $\sigma_y$ , and  $\sigma_{xy}$  on the axes of the material texture coordinate system which is associated with their plastic spin. However, as no experimental data on in-plane uniaxial compression flow stress are available for the steel and aluminum sheets investigated, respectively, by Boehler and Koss [10] and by Truong Qui and Lippmann [43,44], the evaluation of *both* the backstress and the rotation of the material texture frame due to plastic spin in their theory is impossible using solely the experimental data on the directional dependence of uniaxial tensile flow stress. Truong Qui and Lippmann [43,44] used a least-square fitting parameter identification procedure that lumps together all material parameters plus a rotation angle  $\omega_{12}$  due to plastic spin. Such an indirect approach in evaluating the effect of plastic spin and other aspects of a highly nonlinear anisotropic plastic flow behavior is very questionable as noted by McDowell et al. [46]. Alternatively, one may invoke an anisotropic plasticity theory with a nonassociated flow rule, [47], and uses a yield surface to model the anisotropy of flow stress and a separate flow surface to model the anisotropy of plastic strain ratios. Two plastic spins associated with the evolution of symmetry axes of yield and flow surfaces can thus be in principle evaluated independently based on the experimental data on the orientational dependence of flow stress and plastic strain ratio respectively following the methodology give in this investigation. Under this context, the plastic spin ratio obtained here for the two steel sheets should perhaps be limited to the evolution of the yield surface and its applicability to the evolution of the flow surface cannot be assessed without additional experimental data on the orientational dependence of plastic strain ratio.

We take the viewpoint that the purpose of a macroscopic anisotropic plasticity theory is mainly to provide a mathematically more compact but still physically sound description of the plastic flow behavior of a sheet metal so that engineering analyses and designs of sheet metal forming processes can be carried out in an efficient way with accepted accuracy. One basically calibrates the material parameters in the theory through a set of mechanical tests under simple loading conditions and then applies the theory to

analyze problems under more general loading conditions. Our anisotropic plasticity theory formulated in terms of the intrinsic variables of principal stresses and a loading orientation angle intends to strike a proper balance between the mathematical compactness and the descriptive robustness through the truncated Fourier series representation of each of anisotropic material functions characterizing plastic anisotropy of a sheet metal. Depending on the extent of the experimental data made available, the degree of plastic anisotropy, and the accuracy required for an analysis, a flexible and adaptive anisotropic plasticity theory can thus be established for practical engineering applications, [35–40]. There have been some debates in recent years on the role and necessity of macroscopic plastic spin within the framework of a macroscopic polycrystalline plasticity theory [24,46,48]. We suggest that a flow rule of macroscopic plastic spin should be considered if it improves the mathematical formulation (say, the compactness) and the constitutive modeling quality of a phenomenological theory of a sheet metal and if there is a clear physical basis (such as the relative rotation of the material texture frame against the material itself) and an associated experimental procedure for its evaluation. This investigation showed that the proposed flow rule of macroscopic plastic spin can be used to describe effectively the orientational evolution of the material texture frame in three orthotropic sheet metals subjected to off-axis uniaxial tension and thus their plasticity anisotropy without invoking the use of other mathematically more complicated anisotropic hardening models, [43–45]. When other aspects of material texture evolution such as texture spreading or texture sharpening have significant effects on the anisotropic plastic flow behavior of a sheet metal, constitutive anisotropic hardening equations in addition to the flow rule of plastic spin may have to be added to characterize the evolution of texture intensity.

## 5 Conclusions

A new flow rule of macroscopic plastic spin has been proposed for modeling the orientational evolution of the material texture frame of a sheet metal subjected to off-axis uniaxial tension. When a sheet metal has a pre-existing and persisting orthotropic symmetry, the anisotropic material function in the flow rule can be approximated by a truncated Fourier sine series of the loading orientation angle and its Fourier coefficients can be identified using the experimental data on the rotation of the material texture frame relative to the sheet metal itself. The flow rule of macroscopic plastic spin is found to provide a consistent description of the experimental data on the orientational evolution of the material texture frame of three sheet metals reported in the literature. Such a flow rule of macroscopic plastic spin should be incorporated into an anisotropic plasticity theory for finite plastic deformation applications when it can improve both the mathematical formulation (the compactness) and the descriptive quality of the theory and when it can be unambiguously evaluated experimentally based on an explicit mechanistic definition of the material texture frame. Additional theoretical and experimental investigations are needed to clarify the definition of macroscopic plastic spin and its evaluation for a monoclinic sheet metal.

## Acknowledgments

The work reported here was supported in part by a CAREER award to WT from the National Science Foundation (Grant No. CMS-973397, Program Director: Dr. K. Chong). WT would like to acknowledge Profs. John Hutchinson and Jim Rice of Harvard University for their comments that helped to clarify our definition of the material texture frame in a monoclinic sheet.

## Appendix

**On the Micromechanical Basis of the Proposed Anisotropic Plastic Flow Theory.** At ambient conditions, the plastic flow of a single crystal is primarily due to *crystallographic* slips on se-



lected slip systems. The plastic rate of deformation tensor  $\mathbf{D}^p$  and the plastic spin tensor  $\mathbf{W}^p$  of a single crystal can be represented by slip rates associated with slip modes, [49,50]:

$$\begin{aligned}\mathbf{D}^p &= \text{sym}(\mathbf{R}^* \dot{\mathbf{F}}^p \mathbf{F}^{p-1} \mathbf{R}^{*-1}) = \sum_{i=1}^{N^*} \dot{\gamma}_i^* \mathbf{P}_i, \\ \mathbf{W}^p &= \text{skew}(\mathbf{R}^* \dot{\mathbf{F}}^p \mathbf{F}^{p-1} \mathbf{R}^{*-1}) = \sum_{i=1}^{N^*} \dot{\gamma}_i^* \mathbf{Q}_i,\end{aligned}\quad (A1)$$

where  $\mathbf{R}^*$  is the lattice rigid body rotation tensor,  $\mathbf{F}^p$  is the plastic deformation gradient tensor,  $\dot{\gamma}_i^*$  is the absolute value of the rate of change of integrated shear strain for the  $i$ -th crystallographic slip system, and  $N^*$  is the total number of the activated crystallographic slip modes. Each slip mode is composed of a slip direction and a slip plane. The tensors  $\mathbf{P}_i$  and  $\mathbf{Q}_i$  for the  $i$ th slip mode are defined by

$$\begin{aligned}\mathbf{P}_i &= \text{sym} \mathbf{T}_i = \frac{1}{2} (\mathbf{s}_i \otimes \mathbf{m}_i + \mathbf{m}_i \otimes \mathbf{s}_i), \\ \mathbf{Q}_i &= \text{skew} \mathbf{T}_i = \frac{1}{2} (\mathbf{s}_i \otimes \mathbf{m}_i - \mathbf{m}_i \otimes \mathbf{s}_i),\end{aligned}\quad (A2)$$

where the Schmid tensor  $\mathbf{T}_i$  is defined by  $\mathbf{T}_i = \mathbf{s}_i \otimes \mathbf{m}_i$ , and unit vectors  $\mathbf{s}_i$  and  $\mathbf{m}_i$  are the slip direction and normal to the slip plane associated with the  $i$ th slip mode in the deformed configuration, respectively. Activation of the selected slip systems can be prescribed by a certain slip condition. The driving force to activate the  $i$ -th slip system is the resolved shear stress  $\tau_i^*$  along the slip direction on the crystallographic slip plane of the slip system in the current configuration, which can be obtained by  $\tau_i^* = \mathbf{P}_i : \boldsymbol{\sigma}$ , where  $\boldsymbol{\sigma}$  is the Cauchy stress tensor.

We assume the existence of a rate-dependent slip potential  $\tau^*$  (the effective resolved shear stress) for plastic deformation of single crystal grains in a polycrystalline aggregate with a stress exponent  $b (> 1)$

$$\begin{aligned}\tau^*(\tau_1^*, \tau_2^*, \dots, \tau_{N^*}^*) &= [\alpha_1^* |\tau_1^*|^b + \alpha_2^* |\tau_2^*|^b + \dots \\ &+ \alpha_{N^*}^* |\tau_{N^*}^*|^b]^{1/b} = \left[ \sum_{i=1}^{N^*} \alpha_i^* |\tau_i^*|^b \right]^{1/b},\end{aligned}\quad (A3)$$

where  $\tau_i^*$  are resolved shear stresses on the available slip systems of the crystal and  $\alpha_i^*$  are the weight coefficients related to the relative strength of the slip systems. A work-conjugate effective shear rate  $\dot{\gamma}^*$  and the slip surface can be defined as

$$\tau^* \dot{\gamma}^* = \tau_1^* \dot{\gamma}_1^* + \tau_2^* \dot{\gamma}_2^* + \dots + \tau_{N^*}^* \dot{\gamma}_{N^*}^* = \sum_{i=1}^{N^*} \tau_i^* \dot{\gamma}_i^*, \quad (A4)$$

$$\tau^*(\tau_1^*, \tau_2^*, \dots, \tau_{N^*}^*) - \tau_0^*(\xi^*, \dot{\gamma}^*) = 0, \quad (A5)$$

where  $\xi^*$  is a scalar characterizing the overall isotropic hardening of the crystal and  $\tau_0^*(\xi^*, \dot{\gamma}^*)$  is the effective slip strength of the crystal. The associated flow rule results the slip rate on the each slip system as

$$\begin{aligned}\dot{\gamma}_i^* &= \lambda^* \frac{\partial \tau^*(\tau_1^*, \tau_2^*, \dots, \tau_{N^*}^*)}{\partial \tau_i^*} \\ &= \lambda^* \alpha_i^* \left( \frac{|\tau_i^*|}{\tau^*} \right)^{b-2} \frac{\tau_i^*}{\tau^*} \\ &= \dot{\gamma}^* \alpha_i^* \left( \frac{|\tau_i^*|}{\tau^*} \right)^{b-2} \frac{\tau_i^*}{\tau^*} = \dot{\gamma}^* \left( \frac{|\tau_i^*|}{\tau_{i0}^*} \right)^{b-2} \frac{\tau_i^*}{\tau_{i0}^*},\end{aligned}\quad (A6)$$

where  $\lambda^* = \dot{\gamma}^*$  from the plastic work-equivalency requirement (see Eq. (A4)),  $\alpha_i^* = (\tau_{i0}^* / \tau_{i0}^*)^{b-1}$ , and  $\tau_{i0}^* = \tau_{i0}^*(g_i^*, \dot{\gamma}^*)$  is the slip strength on each slip system. Evolution laws of isotropic hardening of the single crystal with  $N^* + 1$  scalar state variables are given as

$$\dot{\xi}^* = \dot{\xi}^*(\dot{\gamma}_1^*, \dot{\gamma}_2^*, \dots, \dot{\gamma}_{N^*}^*), \quad \dot{g}_i^* = \dot{g}_i^*(\dot{\gamma}_1^*, \dot{\gamma}_2^*, \dots, \dot{\gamma}_{N^*}^*). \quad (A7)$$

When one assumes  $b = 1 + m$  (with  $m > 0$ ) and

$$\begin{aligned}\tau_{i0}^*(\xi^*, \dot{\gamma}^*) &= g_i^*(\xi^*) \left( \frac{\dot{\gamma}^*}{\dot{\gamma}_0^*} \right)^{1/m} \quad \text{and} \quad \tau_{i0}^*(g_i^*, \dot{\gamma}^*) \\ &= g_i^* \left( \frac{\dot{\gamma}^*}{\dot{\gamma}_{i0}^*} \right)^{1/m}, \quad \text{so} \quad \alpha_i^* = \left( \frac{\tau_{i0}^*}{\tau_{i0}^*} \right)^m = \left( \frac{\dot{\gamma}_{i0}^*}{\dot{\gamma}_0^*} \right) \left( \frac{g_i^*}{g_i^*} \right)^m,\end{aligned}\quad (A8)$$

one can show that

$$\dot{\gamma}_i^* = \dot{\gamma}^* \left( \frac{|\tau_i^*|}{\tau_{i0}^*} \right)^{m-1} \frac{\tau_i^*}{\tau_{i0}^*} = \dot{\gamma}_{i0}^* \left( \frac{|\tau_i^*|}{g_i^*} \right)^{m-1} \frac{\tau_i^*}{g_i^*}. \quad (A9)$$

This is exactly the rate-dependent slip rule that has been proposed by Hutchinson [51], Asaro [49], and Asaro and Needleman [52]. A combined self-hardening and latent hardening model can be adapted here with  $\xi^* = \gamma_T^*$

$$\dot{g}^* = h^*(\gamma_T^*) \dot{\gamma}_T^*, \quad \dot{g}_i^* = \sum_{j=1}^{N^*} h_{ij}^* \dot{\gamma}_j^*, \quad (A10)$$

where the Taylor strain  $\gamma_T^*$  and the hardening moduli matrix  $h_{ij}^*$  are defined by

$$\gamma_T^* = \sum_{i=1}^{N^*} |\dot{\gamma}_i^*|, \quad h_{ij}^* = q h^* + (1 - q) h^* \delta_{ij}, \quad (A11)$$

where  $q$  is a parameter characterizing the latent hardening. When the latent hardening is equal to the self-hardening ( $q = 1$ ), one has the Taylor isotropic hardening model of single crystals with  $h_{ij}^*(\gamma_T^*) = h^*(\gamma_T^*)$ ,  $\alpha_i^* = 1$ ,  $\xi^* = \gamma_T^*$ , and  $g_i^* = g^*$ . On the other hand, the current crystal plasticity model is a rate-dependent extension of the rate-independent models proposed by Gamin [53] and Darrieulat and Piot [54]. The stress exponent  $b$  has been identified by them respectively as either the interaction exponent of slip systems in a single crystal or the texture dispersion exponent in a polycrystal. This crystal plasticity model with an associated rate-dependent slip potential is more flexible as in general  $b \neq 1 + m$  or  $m \neq \infty$  (where  $m$  is a parameter in a simple power-law rate-dependence model, see Eq. (A8)).

Under uniaxial tension, the resolved shear stresses in terms of the uniaxial tensile stress  $\sigma_\theta > 0$  and the slip system vectors (slip direction and the slip plane normal in terms of the in-plane loading orientation angle  $\theta$ ) are given as

$$\begin{aligned}\tau_i^* &= s_{i1}^{0*} m_{i1}^{0*} \sigma_\theta = L_{i1}^* \sigma_\theta = [s_{i1}^{0*} m_{i1}^{0*} \cos^2 \theta + (s_{i1}^{0*} m_{i2}^{0*} \\ &+ s_{i2}^{0*} m_{i1}^{0*}) \sin \theta \cos \theta + s_{i2}^{0*} m_{i2}^{0*} \sin^2 \theta] \sigma_\theta,\end{aligned}\quad (A12)$$

where  $(s_{i1}^{0*}, s_{i2}^{0*}, s_{i3}^{0*})$  and  $(m_{i1}^{0*}, m_{i2}^{0*}, m_{i3}^{0*})$  are the Cartesian components of the slip system vectors defined in the material texture coordinate system  $XYZ$ . The slip potential Eq. (A3) can be expressed in terms of the uniaxial tensile stress and the in-plane loading orientation angle as

$$\begin{aligned}
[\tau^*(\sigma_\theta, \theta)]^b &= \sigma_\theta^b \sum_{i=1}^{N^*} \alpha_i^* |L_{i1}^*|^b \\
&= \sigma_\theta^b \sum_{i=1}^{N^*} \alpha_i^* |s_{i1}^{0*} m_{i1}^{0*} \cos^2 \theta + (s_{i1}^{0*} m_{i2}^{0*} + s_{i2}^{0*} m_{i1}^{0*}) \\
&\quad \times \sin \theta \cos \theta + s_{i2}^{0*} m_{i2}^{0*} \sin^2 \theta|^b \\
&\equiv \sigma_\theta^b \Phi_1^*(\theta). \tag{A13}
\end{aligned}$$

The in-plane components of the plastic rate of deformation tensor  $\mathbf{D}^p$  and the plastic spin tensor  $\mathbf{W}^p$  of a single crystal can be obtained using Eqs. (A1), (A2), (A6), (A12), and (A13)

$$\begin{aligned}
\dot{\epsilon}_1 &= \sum_{i=1}^{N^*} s_{i1}^* m_{i1}^* \dot{\gamma}_i^* = \dot{\gamma}^* \left( \frac{\sigma_\theta}{\tau_0} \right)^{b-1} \sum_{i=1}^{N^*} \alpha_i^* |L_{i1}^*|^b \\
&\equiv \dot{\gamma}^* \left( \frac{\sigma_\theta}{\tau_0} \right)^{b-1} \Phi_1^*(\theta), \tag{A14a}
\end{aligned}$$

$$\begin{aligned}
\dot{\epsilon}_2 &= \sum_{i=1}^{N^*} s_{i2}^* m_{i2}^* \dot{\gamma}_i^* = \dot{\gamma}^* \left( \frac{\sigma_\theta}{\tau_0} \right)^{b-1} \sum_{i=1}^{N^*} \alpha_i^* |L_{i1}^*|^{b-2} L_{i1}^* L_{i2}^* \\
&\equiv \dot{\gamma}^* \left( \frac{\sigma_\theta}{\tau_0} \right)^{b-1} \Phi_2^*(\theta), \tag{A14b}
\end{aligned}$$

$$\begin{aligned}
\dot{\epsilon}_{12} &= \sum_{i=1}^{N^*} \frac{s_{i1}^* m_{i2}^* + s_{i2}^* m_{i1}^*}{2} \dot{\gamma}_i^* = \dot{\gamma}^* \left( \frac{\sigma_\theta}{\tau_0} \right)^{b-1} \sum_{i=1}^{N^*} \alpha_i^* |L_{i1}^*|^{b-2} L_{i1}^* V_{i1}^* \\
&\equiv \dot{\gamma}^* \left( \frac{\sigma_\theta}{\tau_0} \right)^{b-1} \Phi_3^*(\theta), \tag{A14c}
\end{aligned}$$

$$\begin{aligned}
\dot{\omega}_{12} &= \sum_{i=1}^{N^*} \frac{s_{i1}^* m_{i2}^* - s_{i2}^* m_{i1}^*}{2} \dot{\gamma}_i^* = \dot{\gamma}^* \left( \frac{\sigma_\theta}{\tau_0} \right)^{b-1} \sum_{i=1}^{N^*} \alpha_i^* |L_{i1}^*|^{b-2} L_{i1}^* V_{i2}^* \\
&\equiv \dot{\gamma}^* \left( \frac{\sigma_\theta}{\tau_0} \right)^{b-1} \Phi_4^*(\theta), \tag{A14d}
\end{aligned}$$

where

$$\begin{aligned}
L_{i1}^* &= s_{i1}^* m_{i1}^* = s_{i1}^{0*} m_{i1}^{0*} \cos^2 \theta + (s_{i1}^{0*} m_{i2}^{0*} + s_{i2}^{0*} m_{i1}^{0*}) \sin \theta \cos \theta \\
&\quad + s_{i2}^{0*} m_{i2}^{0*} \sin^2 \theta,
\end{aligned}$$

$$\begin{aligned}
L_{i2}^* &= s_{i2}^* m_{i2}^* = s_{i1}^{0*} m_{i1}^{0*} \sin^2 \theta - (s_{i1}^{0*} m_{i2}^{0*} + s_{i2}^{0*} m_{i1}^{0*}) \sin \theta \cos \theta \\
&\quad + s_{i2}^{0*} m_{i2}^{0*} \cos^2 \theta,
\end{aligned}$$

$$\begin{aligned}
V_{i1}^* &= \frac{s_{i1}^* m_{i2}^* + s_{i2}^* m_{i1}^*}{2} = \frac{s_{i2}^{0*} m_{i2}^{0*} - s_{i1}^{0*} m_{i1}^{0*}}{2} \sin 2\theta \\
&\quad + \frac{s_{i1}^{0*} m_{i2}^{0*} + s_{i2}^{0*} m_{i1}^{0*}}{2} \cos 2\theta,
\end{aligned}$$

$$V_{i2}^* = \frac{s_{i1}^* m_{i2}^* - s_{i2}^* m_{i1}^*}{2} = \frac{s_{i1}^{0*} m_{i2}^{0*} - s_{i2}^{0*} m_{i1}^{0*}}{2}, \quad \text{and}$$

$$\Phi_3^*(\theta) = \frac{1}{2b} \frac{d\Phi_1^*(\theta)}{d\theta} \quad (\text{the associated flow rule}).$$

The material anisotropic functions  $\Phi_1^*(\theta)$ ,  $\Phi_2^*(\theta)$ , and  $\Phi_4^*(\theta)$  of the single crystal under uniaxial tension are related only to its slip system vectors  $\mathbf{s}_i$  and  $\mathbf{m}_i$ , the slip system weight coefficient  $\alpha_i^*$ , and the stress exponent  $b$ . By using the Sachs assumption of the uniform stress field in each single crystal grain of a polycrystal, the macroscopic flow potential and the associated flow rules for plastic strain rates and the flow rule for plastic spin can be

obtained approximately via simple volume averaging. The resulting mathematical formulation of these constitutive equations is identical to the one presented in Section 2 if  $a=b$ .

The plastic spin appeared in the *micromechanical* theory of single crystal plasticity (see Eq. (A1) in general and Eq. (14d) under uniaxial tension) is the natural consequence of the kinematics of crystallographic slips. When one does not directly measure the crystal orientations using either X-ray or electron diffraction techniques, one does not know explicitly the slip system vectors  $\mathbf{s}_i$  and  $\mathbf{m}_i$ . One has to rely on the mechanical tests instead to evaluate the material anisotropic functions  $\Phi_1^*(\theta)$ ,  $\Phi_2^*(\theta)$ , and  $\Phi_4^*(\theta)$  of the single crystal under uniaxial tension. In other words, this results in a *macroscopic* theory of single crystal plasticity using these material anisotropic functions for uniaxial tensile loading. One can show that in general the material anisotropic function  $\Phi_4^*(\theta)$  cannot be deduced from the knowledge of other two anisotropic material anisotropic functions  $\Phi_1^*(\theta)$  and  $\Phi_2^*(\theta)$  for single crystals: that is, the knowledge of the orientational dependence of flow stress and plastic strain ratio under uniaxial tension will not provide any prediction on the orientational dependence of plastic spin ratio at all. Indeed, this result directly contradicts one of the commonly cited expressions for macroscopic plastic spin, [26–28]:

$$\begin{aligned}
\mathbf{W}^p &= \eta(\boldsymbol{\sigma} \mathbf{D}^p - \mathbf{D}^p \boldsymbol{\sigma}), \quad \text{or} \quad \dot{\omega}_{12} \\
&= \eta \sigma_\theta \dot{\epsilon}_{12} \quad (\text{under uniaxial tension}), \tag{A15}
\end{aligned}$$

where  $\eta$  is the plastic spin coefficient (which has been assumed to be a constant in its application examples). Kurroda [26] and Dafalias [28] found that the plastic spin coefficient have to be a negative constant for modeling certain experimental data while it is required to be non-negative according to Levitas [27]. One can show that the relation  $\dot{\omega}_{12} = \eta \sigma_\theta \dot{\epsilon}_{12}$  (uniaxial tension) does not hold for single crystals in general according to the micromechanical crystal plasticity model presented above (numerical simulations of single crystals have revealed that there exist cases that  $\dot{\omega}_{12}$  is nonzero when  $\dot{\epsilon}_{12} = 0$ !) and the general validity of the constitutive equation for macroscopic plastic spin Eq. (A15) is thus questionable. A similar conclusion can also be reached about another proposed simple expression for the macroscopic plastic spin, [28],  $\dot{\omega}_{12} = \eta \dot{\epsilon}_{xy} = \eta[(\dot{\epsilon}_1 - \dot{\epsilon}_2) \sin \theta \cos \theta + \dot{\epsilon}_{12} \cos 2\theta]$  as it holds only strictly for single slips for single crystals.

## References

- [1] Hill, R., 1950, *The Mathematical Theory of Plasticity*, Clarendon Press, Oxford, UK.
- [2] Prager, W., 1955, "The Theory of Plasticity: A Survey of Recent Achievements," *Proc. Inst. Electr. Eng.*, **169**, pp. 41–57.
- [3] Eisenberg, M. A., and Yen, C. F., 1981, "A Theory of Multiaxial Anisotropic Viscoplasticity," *ASME J. Appl. Mech.*, **48**, pp. 276–284.
- [4] McDowell, D. L., 1987, "An Evaluation of Recent Developments in Hardening and Flow Rules for Rate-Independent, Non-Proportional Cyclic Plasticity," *ASME J. Appl. Mech.*, **54**(2), pp. 323–334.
- [5] Hill, R., 1948, "A Theory of the Yielding and Plastic Flow of Anisotropic Metals," *Proc. R. Soc. London, Ser. A*, **193**, pp. 281–297.
- [6] Hill, R., 1979, "Theoretical Plasticity of Textured Aggregates," *Math. Proc. Cambridge Philos. Soc.*, **85**, pp. 179–191.
- [7] Karafillis, A. P., and Boyce, M. C., 1993, "A General Anisotropic Yield Criterion Using Bounds and a Transformation Weighting Tensor," *J. Mech. Phys. Solids*, **41**, pp. 1859–1886.
- [8] Wu, H. C., Hong, H. K., and Shiao, Y. P., 1999, "Anisotropic Plasticity With Application to Sheet Metals," *Int. J. Mech. Sci.*, **41**, pp. 703–724.
- [9] Dawson, P., and Marin, E. B., 1998, "Computational Mechanics for Metal Deformation Process Using Polycrystal Plasticity," *Adv. Appl. Mech.*, **34**, pp. 77–169.
- [10] Boehler, J. P., and Koss, S., 1991, "Evolution of Anisotropy in Sheet-Steels Subjected to Off-Axes Large Deformation," *Advances in Continuum Mechanics*, O. Bruller, V. Mannl, and J. Najjar, eds., Springer, Berlin, pp. 143–158.
- [11] Kim, K. H., and Yin, J. J., 1997, "Evolution of Anisotropy Under Plane Stress," *J. Mech. Phys. Solids*, **45**(5), pp. 841–851.
- [12] Bunge, H. J., and Nielsen, I., 1997, "Experimental Determination of Plastic Spin in Polycrystalline Materials," *Int. J. Plast.*, **13**(5), pp. 435–446.
- [13] Mandel, J., 1974, "Thermodynamics and Plasticity," *Foundations of Continuum Thermodynamics*, J. J. Delgado et al., eds., MacMillan, New York.
- [14] Loree, B., 1983, "On the Effects of Plastic Rotation in the Finite Deformation

- of Anisotropic Elastoplastic Materials," *Mech. Mater.*, **2**, pp. 287–304.
- [15] Dafalias, Y. F., 1984, "The Plastic Spin Concept and a Simple Illustration of Its Role in Finite Plastic Transformations," *Mech. Mater.*, **3**, pp. 223–233.
- [16] Onat, E. T., 1984, "Shear Flow of Kinetically Hardening Rigid-Plastic Materials," *Mechanics of Material Behavior*, G. J. Dvorak and R. T. Shield, eds., Elsevier, New York, pp. 311–324.
- [17] Dafalias, Y. F., 1985, "The Plastic Spin," *ASME J. Appl. Mech.*, **52**, pp. 865–871.
- [18] Dafalias, Y. F., and Rashid, M. M., 1989, "The Effect of Plastic Spin on Anisotropic Material Behavior," *Int. J. Plast.*, **5**, pp. 227–246.
- [19] Dafalias, Y. F., and Aifantis, E. C., 1990, "On the Microscopic Origin of the Plastic Spin," *Acta Mech.*, **82**, pp. 31–48.
- [20] Aravas, E. C., and Aifantis, E. C., 1991, "On the Geometry of Slip and Spin in Finite Plastic Deformation," *Int. J. Plast.*, **7**, pp. 141–160.
- [21] van der Giessen, E., 1992, "A 2D Analytical Multiple Slip Model for Continuum Texture Development and Plastic Spin," *Mech. Mater.*, **13**, pp. 93–115.
- [22] Prantil, V. C., Jenkins, J. T., and Dawson, P. R., 1993, "An Analysis of Texture and Plastic Spin for Planar Polycrystals," *J. Mech. Phys. Solids*, **41**(8), pp. 1357–1382.
- [23] Dafalias, Y. F., 1993, "On Multiple Spins and Texture Development. Case Study: Kinematic and Orthotropic Hardening," *Acta Mech.*, **100**, pp. 171–194.
- [24] Lubarda, V. A., and Shih, C. F., 1994, "Plastic Spin and Related Issues in Phenomenological Plasticity," *ASME J. Appl. Mech.*, **61**, pp. 524–529.
- [25] Schieck, B., and Stumpf, H., 1995, "The Appropriate Corotational Rate, Exact Formula for the Plastic Spin and Constitutive Model for Finite Elastoplasticity," *Int. J. Solids Struct.*, **32**(24), pp. 3643–3667.
- [26] Kuroda, M., 1997, "Interpretation of the Behavior of Metals Under Large Plastic Shear Deformations: A Macroscopic Approach," *Int. J. Plast.*, **13**, pp. 359–383.
- [27] Levitas, V. I., 1998, "A New Look at the Problem of Plastic Spin Based on Stability Analysis," *J. Mech. Phys. Solids*, **46**(3), pp. 557–590.
- [28] Dafalias, Y. F., 2000, "Orientational Evolution of Plastic Orthotropy in Sheet Metals," *J. Mech. Phys. Solids*, **48**, pp. 2231–2255.
- [29] Sidoroff, F., and Dogui, A., 2001, "Some Issues About Anisotropic Elastic-Plastic Models at Finite Strain," *Int. J. Solids Struct.*, **38**, pp. 9569–9578.
- [30] Kuroda, M., and Tvergaard, V., 2001, "Plastic Spin Associated With a Non-Normality Theory of Plasticity," *Eur. J. Mech. A/Solids*, **20**, pp. 893–905.
- [31] Lee, E. H., 1969, "Elastic-Plastic Deformations at Finite Strains," *ASME J. Appl. Mech.*, **36**, pp. 1–6.
- [32] Rice, J. R., 1970, "On the Structure of Stress-Strain Relations for Time-Dependent Plastic Deformation in Metals," *ASME J. Appl. Mech.*, **37**, pp. 728–737.
- [33] Rice, J. R., 1971, "Inelastic Constitutive Relations for Solids: An Internal-Variable Theory and Its Application to Metal Plasticity," *J. Mech. Phys. Solids*, **19**, pp. 433–455.
- [34] Rogers, T. G., 1990, "Yield Criteria, Flow Rules, and Hardening in Anisotropic Plasticity," *Yielding, Damage, and Failure of Anisotropic Solids*, J. P. Boehler, ed., Mechanical Engineering Publications Limited, London, pp. 53–79.
- [35] Tong, W., 2002, "A Planar Plastic Flow Theory of Orthotropic Sheets and the Experimental Procedure for Its Evaluations," *Proc. R. Soc. London, Ser. A*, submitted for publication.
- [36] Tong, W., 2002, "A Plane Stress Anisotropic Plastic Flow Theory for Orthotropic Aluminum Sheet Metals," *Int. J. Plast.*, accepted for publication.
- [37] Tong, W., 2003, "A Planar Plastic Flow Theory for Monoclinic Sheet Metals," *Int. J. Mech. Sci.*, submitted for publication.
- [38] Tong, W., Zhang, N., and Xie, C., 2003, "Modeling of the Anisotropic Plastic Flows of Automotive Sheet Metals," *Aluminum 2003*, S. K. Das, ed., The Minerals, Metals & Materials Society, to appear.
- [39] Tong, W., Xie, C., and Zhang, N., 2003, "Micromechanical and Macroscopic Modeling of Anisotropic Plastic Flows of Textured Polycrystalline Sheets," *Modell. Simul. Mater. Sci. Eng.*, submitted for publication.
- [40] Tong, W., Xie, C., and Zhang, N., 2003, "Modeling the Anisotropic Plastic Flow of Textured Polycrystalline Sheets Using the Generalized Hill's 1979 Non-Quadratic Flow Potential," *Int. J. Plast.*, submitted for publication.
- [41] Hill, R., 1980, "Basic Stress Analysis of Hyperbolic Regimes in Plastic Media," *Math. Proc. Cambridge Philos. Soc.*, **88**, pp. 359–369.
- [42] Hill, R., 1990, "Constitutive Modeling of Orthotropic Plasticity in Sheet Metals," *J. Mech. Phys. Solids*, **38**, pp. 405–417.
- [43] Truong Qui, H. P., and Lippmann, H., 2001, "Plastic Spin and Evolution of an Anisotropic Yield Condition," *Int. J. Mech. Sci.*, **43**, pp. 1969–1983.
- [44] Truong Qui, H. P., and Lippmann, H., 2001, "On the Impact of Local Rotation on the Evolution of an Anisotropic Plastic Yield Condition," *J. Mech. Phys. Solids*, **49**, pp. 2577–2591.
- [45] Losilla, G., Boehler, J. P., and Zheng, Q. S., 2000, "A Generally Anisotropic Hardening Model for Big Offset-Strain Yield Stresses," *Acta Mech.*, **144**, pp. 169–183.
- [46] McDowell, D. L., Miller, M. P., and Bammann, D. J., 1993, "Some Additional Considerations for Coupling of Material and Geometric Nonlinearities for Polycrystalline Metals," *Large Plastic Deformations: Fundamental Aspects and Applications to Metal Forming (MECAMAT'91)*, C. Teodosiu, J. L. Raphanel, and F. Sidoroff, eds., Balkema, Rotterdam, pp. 319–327.
- [47] Stoughton, T. B., 2002, "A Non-Associated Flow Rule for Sheet Metal Forming," *Int. J. Plast.*, **18**, pp. 687–714.
- [48] Dafalias, Y. F., 1998, "The Plastic Spin: Necessity or Redundancy?" *Int. J. Plast.*, **14**, pp. 909–931.
- [49] Asaro, R. J., 1983, "Micromechanics of Crystals and Polycrystals," *Advances in Mechanics*, **23**, p. 1.
- [50] Bassani, J. L., 1994, "Plastic Flow of Crystals," *Advances in Appl. Mech.*, **30**, pp. 191–258.
- [51] Hutchinson, J. W., 1976, "Bounds and Self-Consistent Estimates for Creep of Polycrystalline Materials," *Proc. R. Soc. London, Ser. A*, **348**, pp. 101–127.
- [52] Asaro, R. J., and Needleman, A., 1985, "Texture Development and Strain Hardening in Rate-Dependent Polycrystals," *Acta Metall.*, **33**(6), pp. 923–953.
- [53] Gambin, W., 1992, "Refined Analysis of Elastic-Plastic Crystals," *Int. J. Solids Struct.*, **29**(16), pp. 2013–2021.
- [54] Darrieulat, M., and Piot, D., 1996, "A Method of Generating Analytical Yield Surfaces of Polycrystalline Materials," *Int. J. Plast.*, **12**(5), pp. 575–610.